Adenovirus-mediated gene transfer of endostatin *in vivo* results in high level of transgene expression and inhibition of tumor growth and metastases

Bernhard V. Sauter*, Olivier Martinet*, Wei-Jian Zhang*, John Mandeli†, and Savio L. C. Woo*‡

*Institute for Gene Therapy and Molecular Medicine, and †Department of Biomathematical Sciences, Mount Sinai School of Medicine, New York, NY 10029-6574

Communicated by M. Judah Folkman, Harvard Medical School, Boston, MA, February 15, 2000 (received for review August 10, 1999)

Inhibition of angiogenesis has been shown to be an effective strategy in cancer therapy in mice. However, its widespread application has been hampered by difficulties in the large-scale production of the antiangiogenic proteins. This limitation may be resolved by *in vivo* delivery and expression of the antiangiogenic genes. We have constructed a recombinant adenovirus that expresses murine endostatin that is biologically active both *in vitro*, as determined in endothelial cell proliferation assays, and *in vivo*, by suppression of angiogenesis induced by vascular endothelial growth factor 165. Persistent high serum levels of endostatin (605–1740 ng/ml; mean, 936 ng/ml) were achieved after systemic administration of the vector to nude mice, which resulted in significant reduction of the growth rates and the volumes of JC breast carcinoma and Lewis lung carcinoma ($P < 0.001$ and $P < 0.05$, respectively). In addition, the endostatin vector treatment completely prevented the formation of pulmonary micrometastases in Lewis lung carcinoma ($P = 0.0001$). Immunohistochemical staining of the tumors demonstrated a decreased number of blood vessels in the treatment group versus the controls. In conclusion, the present study clearly demonstrates the potential of vector-mediated antiangiogenic gene therapy as a component in cancer therapy.

antiangiogenesis | cancer | gene therapy

In recent years it has become clear that angiogenesis not only is important in physiological processes such as embryonic development, wound healing, and organ and tissue regeneration, but also plays a pivotal role in tumor progression and metastasis (1). The target of antiangiogenic cancer treatment is the genetically normal endothelial cell. Therefore, the development of resistance to angiostatic therapy is very unlikely and has not been reported so far (2). If a cancer exceeds the size of ≈1–2 mm, recruitment of new blood vessels is needed (angiogenesis) to prevent tumor cell apoptosis. Tumor cells promote angiogenesis by the secretion of angiogenic factors, in particular basic fibroblast growth factor (bFGF) and vascular endothelial growth factor (VEGF) (3). Recently, evidence emerged that angiogenesis is tightly regulated by a balance of activating and inhibiting factors (4). Therefore, continuous overexpression of antiangiogenic factors by gene therapy, for instance, should counteract the tumor-induced angiogenesis.

Many tumor- and non-tumor-associated antiangiogenic factors have been described. The proteolytic cleavage of larger precursor molecules associated with the vascular system (proteins of the coagulation cascade and basement membrane proteins) is thought to play an important role in the generation of several of these antiangiogenic proteins and, thus, in the control of angiogenesis. Of the known angiogenesis inhibitors, the recently discovered protein endostatin, a 20-kDa (184 aa) C-terminal fragment of collagen XVIII, is the most potent inhibitor of tumor angiogenesis described so far (5).

Despite intensive efforts, large quantities of recombinant protein sufficient for clinical trials were not available until recently (6). The difficulties in protein production, long-term storage of bioactive protein, and the cumbersome daily administration may be overcome through transfer of the endostatin gene. Two recent reports using nonviral gene therapy with endostatin show some efficacy against tumor growth (7, 8). The systemic endostatin levels achieved in these studies, however, were rather low. Because there is a dose–response relationship between endostatin concentration and its antiangiogenic effect in all reported *in vitro* and *in vivo* studies, we chose the highly efficient adenovirus-based gene delivery system for our model to maximize transgene expression. Successful antiangiogenic gene therapy with adenoviral vectors already has been shown by several other groups (9–12).

In this paper, we demonstrate the ability to generate persistent high levels of circulating endostatin levels through adenovirus-mediated gene therapy, its effect on tumor growth in two different tumor models [a murine breast cancer cell line (JC) and Lewis lung carcinoma (LLC)], and, more importantly, the complete prevention of lung metastases formation in LLC.

Materials and Methods

Murine Endostatin cDNA Cloning and Adenovirus Construction. Liver tissue from a BALB/c mouse was homogenized, and total RNA was extracted (RNeasy kit; Qiagen, Chatsworth, CA). First-strand cDNA was amplified by reverse transcription–PCR with oligo(dT) primers (SuperScript II; Life Technologies, Grand Island, NY). The full-length mouse endostatin cDNA was amplified by PCR (sense primer with a *Cla*I linker, ATCGATCATACTCATCAGGACTTTCAGCC; antisense primer with a *Not*I linker, GCGGCCGCCTATTTGGAGAAAGAGGTCAT) for subcloning into pBluescript (Stratagene). A synthetic oligonucleotide coding for the rat insulin leader sequence was cloned in front of the endostatin gene. After sequence confirmation, the rat insulin leader endostatin cDNA was cloned into the recombinant adenovirus (ADV) shuttle vector pADV.hEF1-α (human elongation factor 1-α) for the rescue of the recombinant adenovirus as described (13). The viral particles were measured by absorption (A_{260}), and the plaque-forming units (pfu) were determined by standard agarose-overlay plaque assay on 293 cells.

Abbreviations: ADV, recombinant adenovirus; ATTV, average total tumor volume; bFGF, basic fibroblast growth factor; E1, adenovirus early gene 1; GST, glutathione *S*-transferase; HUVEC, human umbilical vein endothelial cells; LLC, Lewis lung carcinoma; moi, multiplicity of infection; pfu, plaque-forming units; VEGF, vascular endothelial growth factor; ICAM-1, intercellular adhesion molecule-1.

‡To whom reprint requests should be addressed at: Institute for Gene Therapy and Molecular Medicine, Box 1496, Mount Sinai School of Medicine, 1425 Madison Avenue, New York, NY 10029-6574. E-mail: swoo@mssm.edu.

The publication costs of this article were defrayed in part by page charge payment. This article must therefore be hereby marked "*advertisement*" in accordance with 18 U.S.C. §1734 solely to indicate this fact.

Article published online before print: *Proc. Natl. Acad. Sci. USA*, 10.1073/pnas.090065597. Article and publication date are at www.pnas.org/cgi/doi/10.1073/pnas.090065597

Recombinant Adenoviruses. All recombinant adenoviruses used in this study were generated in our laboratory as described above. The cDNA for the construction of the ADV.hVEGF165 was obtained through reverse transcription–PCR of RNA isolated from human umbilical vein endothelial cells (HUVEC).

Cell Lines. JC and LLC cell lines were obtained from American Type Culture Collection. The cells were cultured in RPMI medium 1640 (JC) and DMEM (LLC). All media were supplemented with 10% FBS, 0.2 mM glutamine, and 1% penicillin/streptomycin. HUVEC were isolated from umbilical cords (Institutional Review Board-approved cord blood program) by collagenase type IV (Sigma) perfusion (0.2% in Hanks' balanced salt solution) for 20 min at room temperature. The cells then were cultured on collagen-coated (1% in PBS) plates in M199 medium supplemented with 20% FBS, 0.2 mM glutamine, 1% penicillin/streptomycin, and 1 ng/ml bFGF.

Generation of Purified Endostatin. Murine endostatin was cloned into a glutathione *S*-transferase (GST) fusion vector (pGEX-4T-1; Amersham Pharmacia) and expressed in *Escherichia coli* as a 46-kDa GST-endostatin fusion protein. After induction, >90% of the GST-endostatin fusion protein remained in bacterial inclusion bodies. The soluble GST-endostatin fraction was eluted from a 50% slurry of PBS/glutathione-Sepharose 4B (Amersham Pharmacia) with 10 mM reduced glutathione in 50 mM Tris·HCl, pH 8.0. Soluble recombinant endostatin was generated by infection of breast cancer cells with ADV.mEnd at a multiplicity of infection (moi) of 100 pfu. After 48 h, the serum-free supernatant was harvested and sequentially concentrated over Centriplus spin columns (molecular mass cut-off of 50,000 Da followed by 30,000 Da; Amicon). The purified protein was analyzed on a 10% reducing SDS/PAGE gel.

Production of Polyclonal Endostatin Antiserum. The inclusion bodies with GST-endostatin fusion protein were solubilized with 8 M urea and loaded on a preparative SDS/PAGE gel (Protean II; Bio-Rad). The correct-size band was excised and turned over to Research Genetics (Huntsville, AL) for immunization and for the production of polyclonal rabbit anti-endostatin antiserum.

Western Blot of ADV.mEnd Conditioned Supernatant. JC cells were transduced at a moi of 100 pfu with ADV.mEnd and control vector ADV.β-Gal. Conditioned supernatant was harvested after 48 h and concentrated as described above. Samples (5 μl) of the different fractions (50/30-kDa cut-off and flow-through) were separated on a 10% reducing SDS/PAGE gel and transferred to a poly(vinylidene difluoride) membrane (Hybond-P; Amersham Pharmacia). The membrane was probed with the polyclonal rabbit anti-endostatin antiserum, followed by a donkey anti-rabbit FITC-conjugated antibody and a signal amplification step (Vistra Fluorescence Western blotting kit; Amersham Pharmacia). The signals were analyzed with a Storm 860 PhosphorImager (Molecular Dynamics) and IMAGEQUANT software.

***In Vitro* Bioactivity Assay of Endostatin.** Proliferation inhibition assay using a 2-fold dilution series of conditioned supernatant (ADV.mEnd or ADV.β-Gal) on HUVEC was performed as previously described (5). HUVEC proliferation was measured by a tetrazolium-based assay (EZ4U kit; Biomedica, Vienna).

***In Vivo* Angiogenesis Assay.** Athymic nude mice, purchased from the National Cancer Institute, were s.c. injected with 1×10^{11} particles of ADV.hVEGF165 or the adenovirus early gene 1 (E1)-deleted adenovirus control vector ADV.DL312 into an India ink-marked area of the right and left lateral thigh, respectively. The mice were divided into three groups and injected via tail vein with (*i*) PBS, (*ii*) 1×10^{11} ADV.DL312 particles, and (*iii*) 1×10^{11} ADV.mEnd particles. At day 14, the animals were killed, and the marked injection sites on the right and left thighs (ADV.hVEGF165 and ADV.DL312, respectively) were subjected to histological analysis with hematoxylin/eosin staining and immunohistochemistry.

VEGF and Endostatin Measurements. Endostatin levels in conditioned supernatant and serum and human VEGF serum levels were measured with commercially available ELISA kits (CytImmune Sciences, College Park, MD, and R & D Systems).

***In Vivo* Evaluation of Tumor Growth.** Cells (1×10^5 LLC or JC) were inoculated s.c. into nude mice. Tumors were measured with calipers in two dimensions every 4 to 5 days, and the volume was calculated as length $\times$ width$^2 \times 0.52$.

Immunohistochemistry. Sections were probed with a monoclonal rat anti-mouse intercellular adhesion molecule-1 (ICAM-1) antibody (1:300; Seikagaku America, Rockville, MD), followed by a biotinylated polyclonal rabbit anti-rat antibody (1:100; Vector Laboratories).

Statistical Analyses. For comparison of individual time points, ANOVA and unpaired Student's *t* tests were used. For each animal, the average total tumor volume (ATTV) was calculated from the first tumor measurement to the end of the experiment. The ATTV equals the area under the curve (AUC) of the tumor volumes over time divided by the number of days [e.g., ATTV = AUC/number of days = AUC/(26 − 7) = AUC/19]. The ATTV represents the average height of the volume–time curve from day 6 to day 27, thereby giving an overall index of tumor size. *P* values were calculated by using the Wilcoxon Rank Sum Test (14).

Results

Construction of a Recombinant Adenovirus Expressing Murine Endostatin. The cDNA of murine endostatin was PCR-cloned from a mouse liver, and a synthetic oligonucleotide coding for the rat insulin leader sequence was added at the 5′ end. The recombinant replication-deficient adenovirus was generated through cotransfection of the expression cassette containing an adenovirus shuttle vector with an E1-deleted adenovirus backbone vector (pJM-17) (Fig. 1*A*). A restriction digestion of viral DNA with *Hin*dIII was performed to verify the rearrangement of restriction fragments of ADV.mEnd DNA compared with the backbone adenoviral vector plasmid, confirming the correct insertion of the transgene. Aside from minor band shifts, the loss of the 3,437-bp DNA fragment in the recombinant virus as compared with the plasmid is the hallmark of transgene insertion into the E1 region of the adenovirus (Fig. 1*B*). A murine breast cancer cell line with a high transduction efficiency by adenovirus was transduced with an moi of 100 pfu of ADV.mEnd or ADV.β-Gal, respectively, and serum-free supernatant was sequentially concentrated over two columns with a molecular mass cut-off of 50 kDa followed by 30 kDa. Then, 5 μl of the concentrated supernatant was separated on a reducing 10% SDS/PAGE gel, and a distinct band at around 22 kDa was visualized in the ADV.mEnd conditioned supernatant but not in the control. The 22-kDa band, corresponding to the size of endostatin, was seen in both the 50-kDa and the 30-kDa cut-off fractions but not in the flow-through of the 30-kDa column, indicating that protein charges and conformation influenced its filtration through the membranes. Incomplete reduction of multimers and association with other cellular proteins in this highly overexpressed system may have accounted for the retention in the 50-kDa cut-off column (Fig. 1*C*). Polyclonal rabbit anti-endostatin antibody, raised against a GST-endostatin fusion

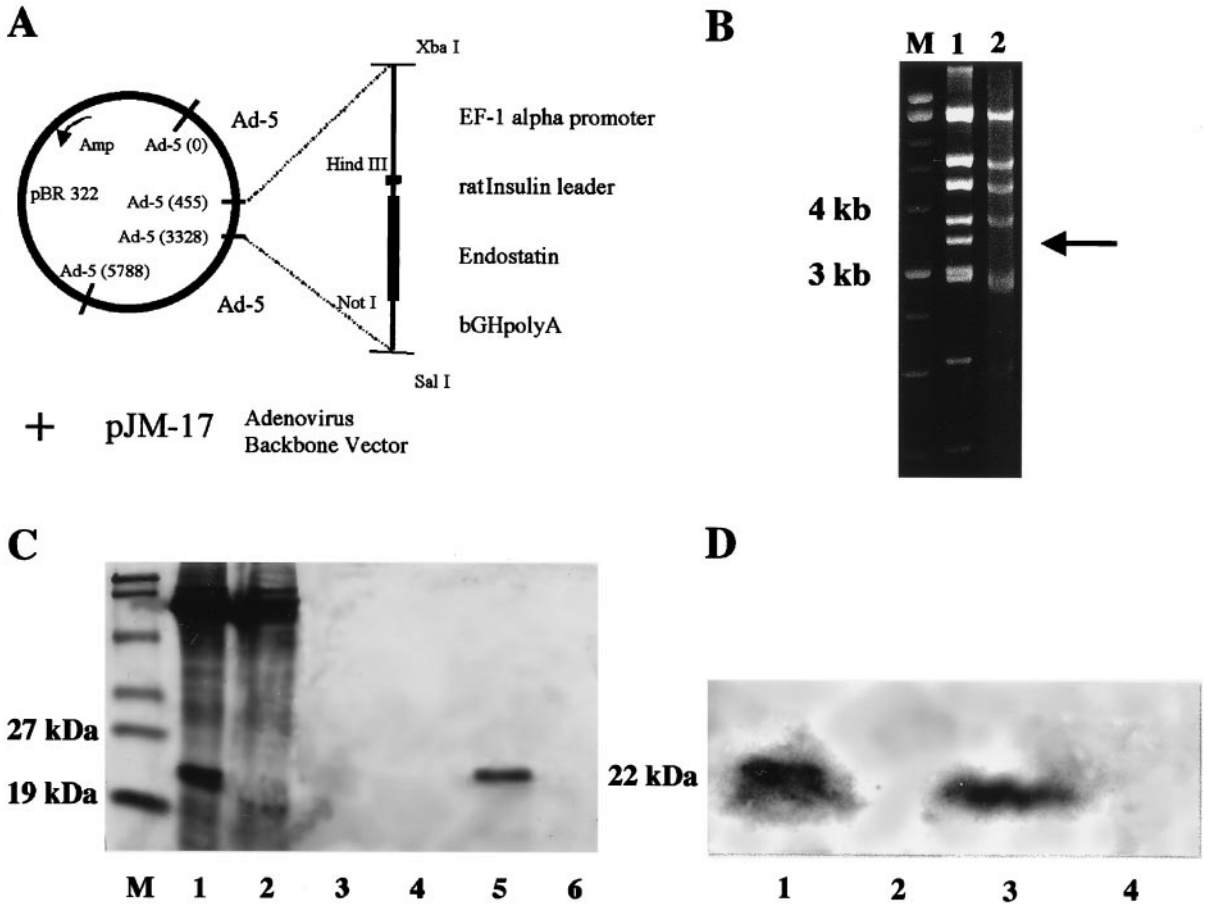

Fig. 1. Construction, molecular analysis, and transgene expression of ADV.mEnd. (*A*) The expression cassette consisting of human elongation factor-1 α (EF-1α) promoter, the rat insulin leader sequence, the cDNA of murine endostatin, and the bovine growth hormone poly(A) (bGHPA) was cloned in an adenovirus shuttle vector. Recombinant adenovirus was generated on cotransfection of the shuttle plasmid with the adenovirus backbone plasmid pJM-17. (*B*) Rearrangement of *Hin*dIII restriction fragments (loss of a 3,437-bp fragment (arrow), emergence of a 1,003-bp fragment (data not shown), and other minor band shifts of the adenovirus backbone plasmid (lane 1) as compared with the recombinant ADV.mEnd (lane 2) confirmed the correct insertion of the transgene into the E1 region in the adenovirus. (*C*) Ten percent reducing SDS/PAGE of serum-free concentrated supernatant of virally transduced breast cancer cells. Retention on 50-kDa molecular mass cut-off column, ADV.mEnd (lane 1) and ADV.β-Gal (lane 2); flow-through of 30-kDa cut-off column, ADV.mEnd (lane 3) and ADV.β-Gal (lane 4); retention on 30-kDa molecular mass cut-off column, ADV.mEnd (lane 5) and ADV.β-Gal (lane 6). (*D*) Western blot of the same supernatant as shown in *C*. Lanes 1 and 2 are the same as in *C*, and lanes 3 and 4 correspond to lanes 5 and 6 in *C*. M, molecular mass markers.

protein, reacted positively in a Western blot with the 22-kDa protein only. Preimmune serum in all fractions and immune serum against conditioned medium of the control vector did not generate any signals, thereby confirming both the specificity of the anti-endostatin antibody and that endostatin is efficiently secreted into the supernatant of ADV.mEnd-transduced cells (Fig. 1*D*).

ADV.mEnd-Expressed Endostatin Is Biologically Active *in Vitro* and *in Vivo*. To evaluate the biological function of the recombinant endostatin, we tested the purified protein from serum-free concentrated supernatant of adenovirally transduced cells in a proliferation inhibition assay on HUVEC. A dose–response between endostatin concentration and percentage inhibition of bFGF-stimulated HUVEC proliferation could be demonstrated (Fig. 2*A*). The ED_{50} of endostatin (975 ng/ml) was in the range of previously published data (15), but was a little higher than in the original paper (5). Similarly, nonconcentrated conditioned supernatant of JC cells transduced with ADV.mEnd strongly inhibited HUVEC proliferation with an ED_{50} at a dilution of 1:16, whereas ADV.β-Gal conditioned supernatant did not inhibit proliferation (Fig. 2*B*). As measured by a commercially available ELISA, endostatin concentration in the conditioned supernatant ranged from 12 to 16 μg/ml. There was no effect of purified endostatin or conditioned supernatant on the growth of JC cells (data not shown).

In vivo antiangiogenic activity of adenovirally expressed endostatin was tested by s.c. injection of 1×10^{11} particles of ADV.hVEGF165 or ADV.DL312 into India ink-marked areas of the right and left lateral thighs of a nude mouse, respectively. Particles (1×10^{11}) of ADV.mEnd or ADV.DL312, or PBS was then administered systemically through the tail vein. The left ADV.DL312-injected thigh served as an internal control in each mouse for potential local, nonspecific adenoviral effects. Mice were killed 14 days after viral injection, and the marked area was examined histologically. Histological sections were stained with hematoxylin/eosin and for ICAM-1. There was a clear inhibition of VEGF165-induced angiogenesis in the ADV.mEnd-treated mice vs. the mice injected with the control vector (Fig. 3). ADV.mEnd treatment resulted in endostatin levels from 625 to 1612 ng/ml. There was no increase in systemic angiogenesis as evidenced by the lack of detectable serum levels of human VEGF and by the absence of increased angiogenesis in the contralateral ADV.DL312-injected thigh (data not shown).

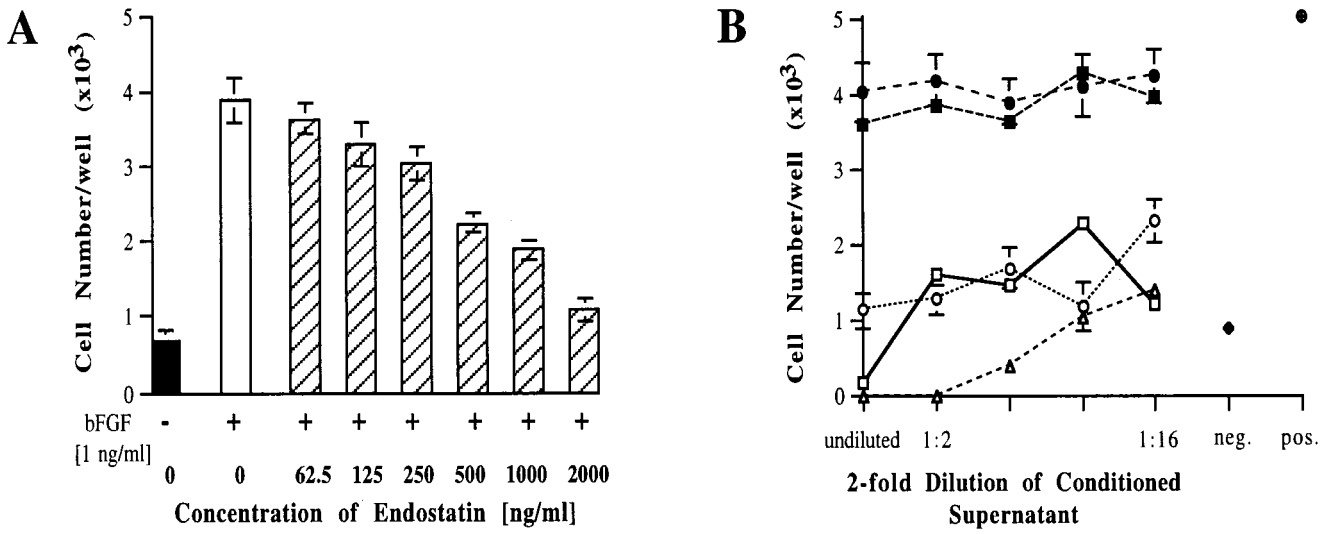

Fig. 2. *In vitro* assay for endostatin activity. (*A*) Inhibition of bFGF (1 ng/ml) stimulated HUVEC proliferation by increasing amounts of purified, ADV.mEnd-expressed endostatin (hatched columns) and in the absence of endostatin (positive control; open column). HUVEC proliferation without bFGF (negative control; filled column). (*B*) Same assay as in *A*. Shown is a 2-fold dilution of conditioned supernatant of JC cells transduced with ADV.mEnd or ADV.β-Gal at different moi (in particles). ADV.mEnd: 1×10^4 (○), 5×10^4 (□), and 1×10^5 (△). ADV.β-Gal: 1×10^4 (●) and 5×10^4 (■). pos., Complete medium with bFGF; neg., complete medium without bFGF. Data are shown as the mean of six wells. Bars indicate ± SD.

Systemic ADV.mEnd Administration Significantly Delays Tumor Engraftment. In the first *in vivo* experiment, we asked whether systemic administration of ADV.mEnd could prevent the formation of s.c. breast cancer (JC) in nude mice. Particles (1×10^{11}) of ADV.mEnd or control vector (ADV.DL312) were injected i.v. into the tail vein, followed by s.c. tumor-cell implantation (1×10^5 cells) 2 days later (20 animals per group). Animals were checked daily, and the emerging tumors were measured twice a week. By day 12 after tumor implantation, a statistically significant difference could be observed between treated and control groups ($P = 0.014$), with four animals in each group not having developed a tumor. Eventually, all animals developed tumors, but the growth rate of the ADV.mEnd-treated group was significantly slower than that in the controls, resulting in a 60% tumor size reduction in the treatment group at day 28 ($P = 0.0008$) (Fig. 4). Endostatin levels ranged from 810 to 1740 ng/ml in the treatment group and from 178 to 190 ng/ml in the control group.

ADV.mEnd Treatment Reduces Tumor Growth and Prevents Metastases. In a more clinically relevant situation, we treated preestablished tumors with ADV.mEnd. As a tumor model, we chose LLC for its general resistance to conventional tumor therapies, according to the National Cancer Institute screening panel for anticancer drugs. LLC cells (1×10^5) were inoculated s.c., and after establishment of a sizable tumor after 7 days (mean tumor volume, 47 mm^3; range, 28–64 mm^3), recombinant adenovirus was injected i.v. by tail vein (in nine treatment and seven control animals). A significant tumor reduction in the treatment group was already seen at day 6 after virus injection ($P = 0.048$). At day 26, when the control animals had to be killed for tumor burden, the decrease in tumor volume for the endostatin group reached

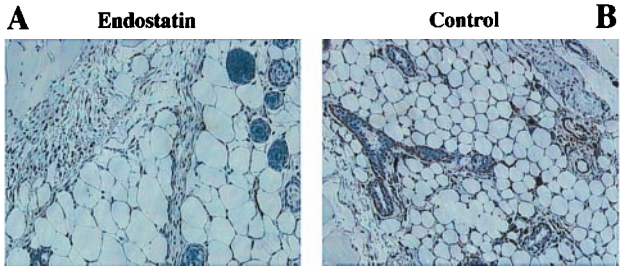

Fig. 3. *In vivo* assay for activity of ADV.mEnd-expressed endostatin. An adenovirus expressing hVEGF165 was injected s.c. into nude mice. At the same time, ADV.mEnd or control vector (ADV.DL312) was administered through the tail vein. After 14 days, the animals were killed, and the ADV.hVEGF165 injection site was histologically analyzed. ICAM-1 staining shows no s.c. blood vessels in the ADV.mEnd-treated animals (*A*) but showed increased angiogenesis in the ADV.DL312-treated animals (*B*). (×100.)

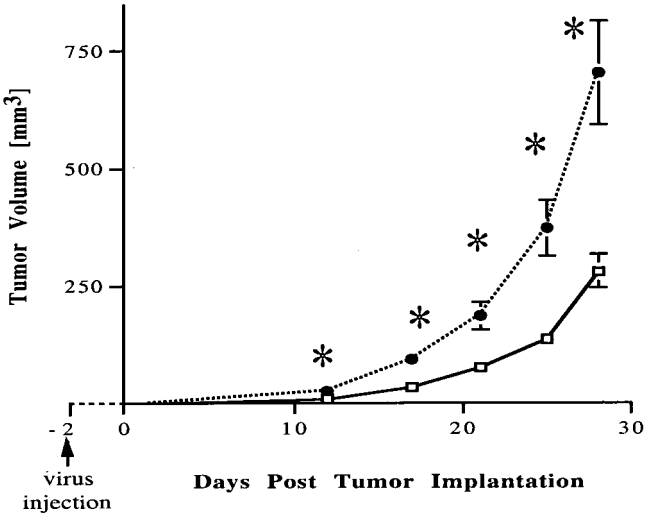

Fig. 4. Delay of tumor engrafting by ADV.mEnd. Recombinant adenovirus was injected i.v. 2 days before s.c. implantation of 1×10^5 JC cells. At 12 days after tumor implantation, a statistically significant difference in tumor size ($P = 0.01$) between the ADV.mEnd-treated (□) and the control vector-treated (ADV.DL312, ●) groups was observed. Tumor volume reduction at day 28 was 60% for the treatment group vs. controls ($P = 0.0008$). *, Statistically significant at the $P = 0.01$ level by unpaired Student's *t* test. Overall index of tumor size, median ATTV: ADV.mEnd, 88 mm^3; ADV.DL312, 190 mm^3. $P = 0.003$ (Wilcoxon rank sum test). There were 20 mice per group. Bars indicate ± SEM.

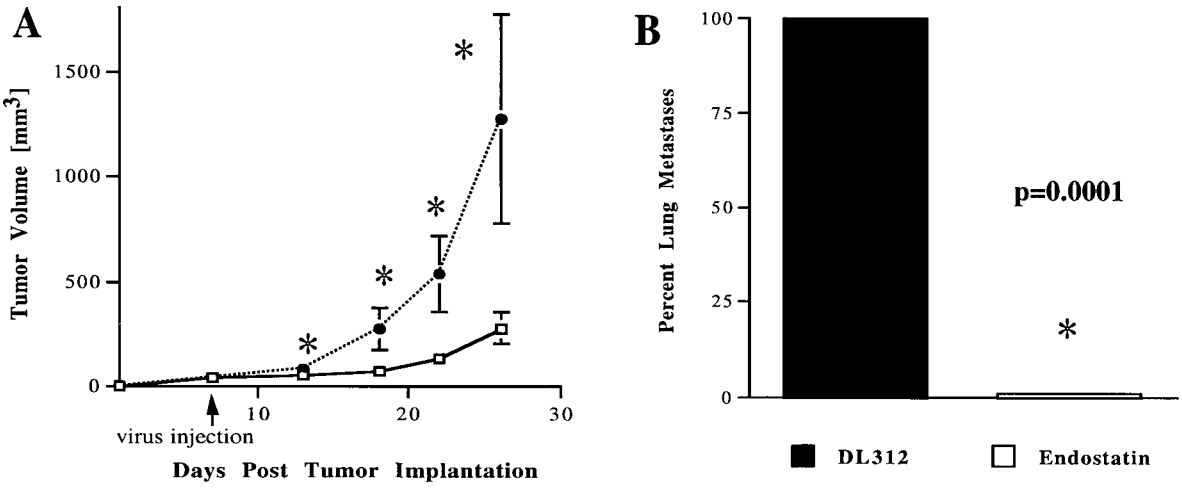

Fig. 5. ADV.mEnd treatment reduces tumor growth of preestablished tumors and prevents formation of lung metastases. LLC cells (1×10^5) were injected s.c. into nude mice. Virus treatment by tail vein injection was given at day 7 (mean total volume, 47 mm^3). (*A*) At 6 days after virus injection, the tumors in the endostatin group (□; nine mice) were already significantly smaller than the controls (●; seven mice). At day 26, the total volume reduction was 78% for the treatment group vs. controls (P = 0.041). ∗, Statistically significant at the $P = 0.05$ level by unpaired Student's *t* test. Overall index of tumor size, median ATTV: ADV.mEnd, 96 mm^3; ADV.DL312, 208 mm^3. $P = 0.05$ (Wilcoxon rank sum test). (*B*) None of the ADV.mEnd-treated mice had lung micrometastases as opposed to 100% of the ADV.DL312-treated controls who did ($P = 0.0001$, Fisher's exact test).

78% ($P = 0.041$) (Fig. 5*A*). Moreover, histological analysis of the lungs of the LLC-bearing animals revealed that none of the nine ADV.mEnd-treated animals developed lung micrometastases, whereas all control animals were found to have tumor in the lungs ($P = 0.0001$; Fig. 5*B*). Endostatin serum levels were similar as in the above experiments with 605-1524 ng/ml after treatment with ADV.mEnd and 165–178 ng/ml in the control group.

Persistent High Serum Levels of Endostatin After a Single Injection of ADV.mEnd. Mean serum endostatin levels, including all of the tumor-bearing mice, were 936 ng/ml (range, 605-1740 ng/ml) at 26–28 days after injection of ADV.mEnd and 176 ng/ml (range, 165–190 ng/ml) for the ADV.DL312-treated groups ($P < 0.0001$) at the same time period.

ADV.mEnd Reduces Tumor-Induced Angiogenesis. Histological analysis by standard hematoxylin/eosin staining and immunohistochemistry with ICAM-1 of both the LLC and JC tumors showed decreased vascularization in the ADV.mEnd-treated animals (Fig. 6). A striking induction of angiogenesis was especially observed directly at the interface of the tumor and the surrounding s.c. tissue in the control vector-treated JC tumors (Fig. 6D_1).

Discussion

We have constructed a recombinant adenovirus expressing biologically active murine endostatin (ADV.mEnd) as shown in both *in vitro* and *in vivo* models of angiogenesis. Treatment of tumor-bearing nude mice with ADV.mEnd led to a tumor volume reduction of up to 78% as compared with the controls and, more importantly, completely prevented the formation of lung metastases in an LLC model. Histological data demonstrated decreased tumor vascularization and less angiogenesis around the tumor in the endostatin-treated animals. Difficulties in large-scale production of recombinant endostatin have been hampering the transition to clinical trials. Only recently, a more efficient production system of soluble endostatin in *Pichia pastoris* was reported (6). However, the challenge of the long-term storage of bioactive protein and the cumbersome daily administration remain. In this paper, we demonstrated that a single injection of ADV.mEnd resulted in persistent high endostatin serum levels (936 ng/ml), more than 30 times higher

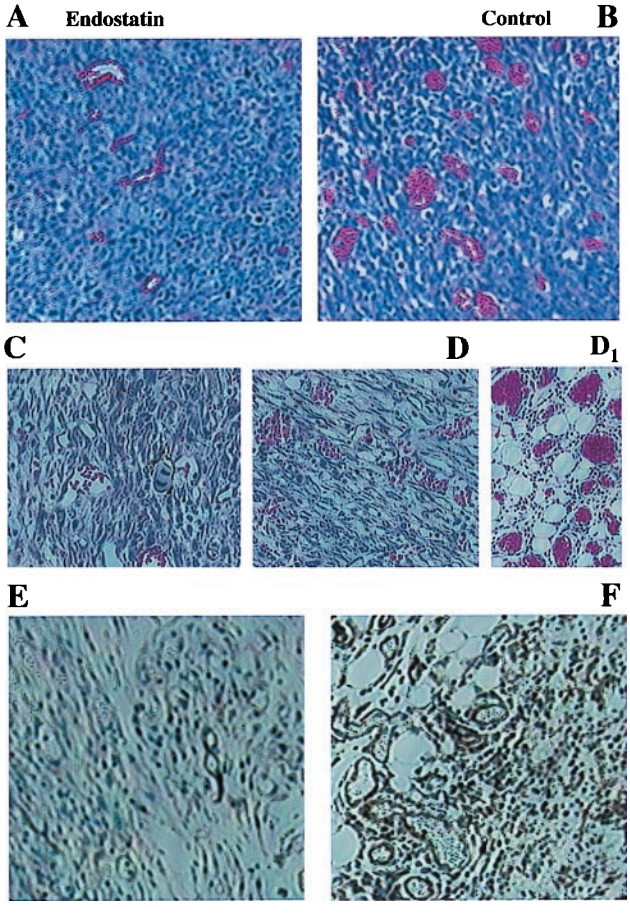

Fig. 6. Reduced angiogenesis in ADV.mEnd-treated tumors. (*A–F*) Decreased tumor vascularization could be demonstrated in all ADV.mEnd-treated tumors [LLC, hematoxylin/eosin (*A*); JC, hematoxylin/eosin (*C*); JC, ICAM-1 (*E*)] as compared with the controls [LLC, hematoxylin/eosin (*B*); JC, hematoxylin/eosin (*D*); JC, ICAM-1 (*F*)]. (D_1) Markedly increased angiogenesis also could be observed at the border zone between tumor and surrounding tissue in the control group of the JC tumors. (*A–F*, ×100; D_1, ×200.)

than previously was reported with nonviral endostatin gene therapy (7, 8). The activity (ED_{50}) of ADV.mEnd-expressed and purified endostatin in endothelial cell proliferation assays was similar (15) or slightly lower (5) than that of endostatin obtained through other expression systems. Higher endostatin activity of recombinant endostatin was reported in only one paper, where a different *in vitro* assay (endothelial cell migration) and *in vivo* administration (peritumoral) were used (16). The adenovirus-mediated delivery of endostatin was clearly superior (much higher transgene expression levels, treatment of larger preestablished tumors, and complete prevention of metastases) to the reported plasmid-based, nonviral gene transfer methods (direct i.m. injection or liposome complexed) (7, 8). A positive correlation between endostatin dose and inhibition of endothelial cell proliferation *in vitro* has been demonstrated (5, 17). Furthermore, it also has been reported that levels of <1 μg/ml endostatin did not induce endothelial cell apoptosis *in vitro* (17). Thus, the better therapeutic effect of the endostatin protein treatment as compared with the ADV.mEnd therapy may be caused by still insufficient expression levels of endostatin (≈ 1 μg/ml) by the adenovirus. Serum levels of endostatin after protein therapy have not been reported thus far. However, the effective dose of recombinant endostatin protein for tumor inhibition (10–20 mg/kg per day) results probably in higher circulating endostatin levels than reported here, even when the relatively short half-life of the protein is taken into account.

As recently shown in a transgenic multistage model of carcinogenesis, endostatin was not able to prevent the transition from large adenomas into the invasive carcinoma stage (18). This occurrence could be the reason that, despite the early statistically significant treatment effect of ADV.mEnd (6 days after virus injection), insufficient endostatin levels may have allowed a number of cells to "escape" from therapy and to enter an invasive state where endostatin was not effective anymore. As previously demonstrated, lung metastases could be inhibited very effectively with a 50 times lower dose of recombinant endostatin (0.3 mg/kg) than that used for tumor treatment (5). Therein may be the explanation as to why the ADV.mEnd-generated endostatin levels, albeit not high enough to induce regression of preestablished tumors, were sufficient to completely prevent the engraftment of circulating tumor cells to form lung micrometastases. In contrast, only a partial effect on metastases was observed when a low-expression gene delivery system was used (7). This finding provides important information, especially for potential clinical applications, on the impact of endostatin serum concentrations on primary tumors and metastases.

Circulating endostatin levels, however, may not be the only explanation for the difference between therapy with endostatin protein and with ADV.mEnd, because angiogenesis is a complex process involving proteolytic basement membrane degradation as well as loss of adhesion, migration, and proliferation of endothelial cells. Different tissue deposition patterns between the s.c. administered protein, and the mostly hepatically produced and secreted endostatin by adenovirus gene therapy may play a role in the control of tumor angiogenesis, because it has been suggested that tissue saturation at the tumor site after repetitive treatments could also be an important factor (2, 19). Despite the known facts about endostatin [crystal structure (20), induction of endothelial cell apoptosis (21), interaction with other extracellular matrix proteins (22) and heparan sulfate (23), and some mutational analyses (15, 16, 24)], much of the molecular mechanism of its action, including the role of zinc (16, 24), remains elusive.

In summary, we showed that high circulating levels of biologically active endostatin could be achieved through adenovirus-mediated gene transfer. To increase the efficacy of endostatin gene therapy, however, an increase of transgene expression levels by choosing different promoters/enhancers and/or by generation of fusion proteins to prolong the endostatin half-life are needed. Further studies on the molecular mechanism of endostatin may also provide new insights that could be explored for endostatin gene therapy. Finally, a gutless, nonimmunogenic, and less toxic adenovirus system that was shown to permit stable long-term transgene expression in monkeys would have to be explored for potential human trials (25). In the present form, endostatin gene therapy does not provide a cure for cancer; however, it may be very useful in conjunction with other cancer treatment modalities.

We thank Drs. S.-H. Chen and S. Hall for helpful discussions. This work was funded in part by the Department of Defense 17-99-1-9307 and by awards from Novartis, Inc., and Hoffmann–La Roche, Inc. (to B.V.S.).

1. Hanahan, D. & Folkman, J. (1996) *Cell* **86,** 353–364.
2. Boehm, T., Folkman, J., Browder, T. & O'Reilly, M. S. (1997) *Nature (London)* **390,** 404–407.
3. Folkman, J. & D'Amore, P. A. (1996) *Cell* **87,** 1153–1155.
4. Folkman, J. (1995) *N. Engl. J. Med.* **333,** 1757–1763.
5. O'Reilly, M. S., Boehm, T., Shing, Y., Fukai, N., Vasios, G., Lane, W. S., Flynn, E., Birkhead, J. R., Olsen, B. R. & Folkman, J. (1997) *Cell* **88,** 277–285.
6. Boehm, T., Pirie-Shepherd, S., Trinh, L. B., Shiloach, J. & Folkman, J. (1999) *Yeast* **15,** 563–572.
7. Blezinger, P., Wang, J., Gondo, M., Quezada, A., Mehrens, D., French, M., Singhal, A., Sullivan, S., Rolland, A., Ralston, R. & Min, W. (1999) *Nat. Biotechnol.* **17,** 343–348.
8. Chen, Q. R., Kumar, D., Stass, S. A. & Mixson, A. J. (1999) *Cancer Res.* **59,** 3308–3312.
9. Griscelli, F., Li, H., Bennaceur-Griscelli, A., Soria, J., Opolon, P., Soria, C., Perricaudet, M., Yeh, P. & Lu, H. (1998) *Proc. Natl. Acad. Sci. USA* **95,** 6367–6372.
10. Goldman, C. K., Kendall, R. L., Cabrera, G., Soroceanu, L., Heike, Y., Gillespie, G. Y., Siegal, G. P., Mao, X., Bett, A. J., Huckle, W. R., *et al*. (1998) *Proc. Natl. Acad. Sci. USA* **95,** 8795–8800.
11. Lin, P., Buxton, J. A., Acheson, A., Radziejewski, C., Maisonpierre, P. C., Yancopoulos, G. D., Channon, K. M., Hale, L. P., Dewhirst, M. W., George, S. E. & Peters, K. G. (1998) *Proc. Natl. Acad. Sci. USA* **95,** 8829–8834.
12. Kong, H. L., Hecht, D., Song, W., Kovesdi, I., Hackett, N. R., Yayon, A. & Crystal, R. G. (1998) *Hum. Gene Ther.* **9,** 823–833.
13. Bautista, D. S., Hitt, M., McGrory, J. & Graham, F. L. (1991) *Virology* **182,** 578–596.
14. Sklarin, N. T., Chahinian, A. P., Feuer, E. J., Lahman, L. A., Szrajer, L. & Holland, J. F. (1988) *Cancer Res.* **48,** 64–67.
15. Dhanabal, M., Ramchandran, R., Volk, R., Stillman, I. E., Lombardo, M., Iruela-Arispe, M. L., Simons, M. & Sukhatme, V. P. (1999) *Cancer Res.* **59,** 189–197.
16. Yamaguchi, N., Anand-Apte, B., Lee, M., Sasaki, T., Fukai, N., Shapiro, R., Que, I., Lowik, C., Timpl, R. & Olsen, B. R. (1999) *EMBO J.* **18,** 4414–4423.
17. Dhanabal, M., Volk, R., Ramchandran, R., Simons, M. & Sukhatme, V. P. (1999) *Biochem. Biophys. Res. Commun.* **258,** 345–352.
18. Bergers, G., Javaherian, K., Lo, K. M., Folkman, J. & Hanahan, D. (1999) *Science* **284,** 808–812.
19. Black, W. R. & Agner, R. C. (1998) *Nature (London)* **391,** 450 (lett.).
20. Hohenester, E., Sasaki, T., Olsen, B. R. & Timpl, R. (1998) *EMBO J.* **17,** 1656–1664.
21. Dhanabal, M., Ramchandran, R., Waterman, M. J., Lu, H., Knebelmann, B., Segal, M. & Sukhatme, V. P. (1999) *J. Biol. Chem.* **274,** 11721–11726.
22. Sasaki, T., Fukai, N., Mann, K., Gohring, W., Olsen, B. R. & Timpl, R. (1998) *EMBO J.* **17,** 4249–4256.
23. Chang, Z., Choon, A. & Friedl, A. (1999) *Am. J. Pathol.* **155,** 71–76.
24. Boehm, T., O'Reilly, M. S., Keough, K., Shiloach, J., Shapiro, R. & Folkman, J. (1998) *Biochem. Biophys. Res. Commun.* **252,** 190–194.
25. Morral, N., O'Neal, W., Rice, K., Leland, M., Kaplan, J., Piedra, P. A., Zhou, H., Parks, R. J., Velji, R., Aguilar-Cordova, E., *et al*. (1999) *Proc. Natl. Acad. Sci. USA* **96,** 12816–12821.